SAE INTERNATIONAL

ARTICLE INFO
Article ID: 03-17-06-0045

doi:10.4271/03-17-06-0045

The Hybrid Concept of Turboshaft Engine Enhanced by Steam Cycle Using Waste Heat Recovery—Combined Analytical and Numerical Calculation of Its Efficiency

***Piotr Tarnawski*[1] *and Wiesław Ostapski*[1]**

[1]*Warsaw University of Technology, Institute of Machine Design Fundamentals, Poland*

Abstract

The article presents a hybrid concept of a turboshaft engine that fits into the area of PGE (pressure-gained combustion). It combines the advantages and elements of a piston engine and a turbine engine. The combustion takes place in isochoric chambers. The proposed timing system of the engine efficiently realizes the Humphrey cycle. Additionally, the main gas cycle engine was enhanced by the Clausius–Rankine steam cycle to achieve effective power of engine equal to 1231.3 kW. It was supplied by waste heat recovery from the exhaust gas. The enhancement of the engine by the secondary steam cycle significantly improved engine effective efficiency with a final value reaching 0.446. The effective efficiency and specific fuel consumption of the engine were calculated using merged analytical–numerical CFD (computational fluid dynamics) analysis. The centrifugal compressor, gas turbine, and steam turbine can work on the common shaft whose rotational velocity is 35,000 rpm. Because of additional weight, it could have potential applications for stationary use or heavy military units.

History

Received: 03 Jan 2024
Revised: 29 Feb 2024
Accepted: 21 May 2024
e-Available: 04 Jun 2024

Keywords

Pressure-gained combustion, Humphrey cycle, Turboshaft engine, CFD analysis, Valve timing system, Sealing system, Combined cycle gas turbine, Engine efficiency, Waste heat recovery

Citation

Tarnawski, P. and Ostapski, W., "The Hybrid Concept of Turboshaft Engine Enhanced by Steam Cycle Using Waste Heat Recovery—Combined Analytical and Numerical Calculation of Its Efficiency," *SAE Int. J. Engines* 17(6):795-806, 2024, doi:10.4271/03-17-06-0045.

ISSN: 1946-3936
e-ISSN: 1946-3944

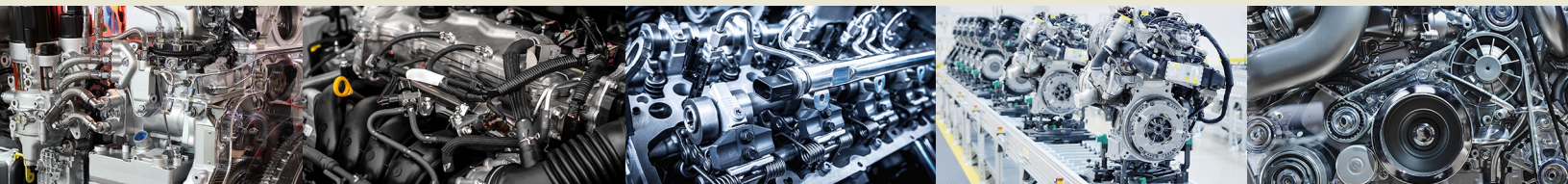

1. Introduction

An improvement in the effective efficiency of the engine enables lower emission of toxins into the atmosphere, as well as better performance of the vehicle, which has primary importance, especially in military applications [1, 2].

Intensely investigated by authors, the possibility of the application of isochoric combustion to a turbine engine [3, 4, 5, 6, 7, 8, 9] led to the creation of the hybrid concept of a turboshaft engine. Figure 1 presents a variant with a partial turbine load, and Figure 2 presents a variant with an entire turbine load. It works according to the Humphrey cycle, in which the efficiency of the thermodynamic cycle is better than the Bryton–Joule cycle (based on which works a classical turbine engine). For pressure ratio 18 and 1.5 MJ/kg of added heat the theoretical Bryton–Joule cycle has an efficiency equal to 0.56, but the Humphrey cycle has an efficiency equal to 0.66. The application of the Humphrey cycle gives the potential advantage of 18% relative to the Bryton–Joule cycle [9]. The reason for this is the pressure increase during combustion for the Humphrey cycle (see comparison of both cycles in Figure 3).

The proposed engine concept has common elements of a turbine and a piston engine hence the name hybrid engine. For example, it has a temporarily closed combustion chamber, which is supplied by fuel direct injection systems.

FIGURE 1 Geometry model of the hybrid concept of turboshaft engine with partial turbine load—1000 kW (general and top view).

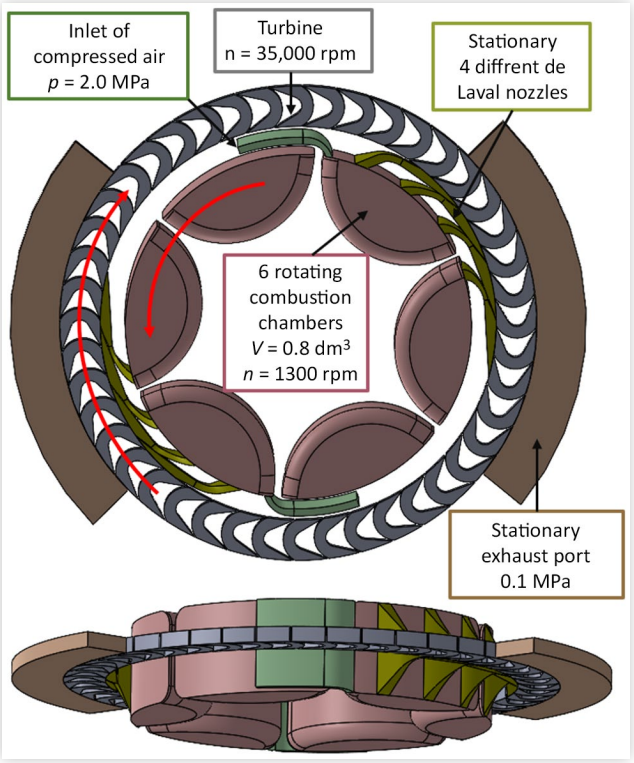

FIGURE 2 Geometry model of the hybrid concept of turboshaft engine with entire turbine load—1800 kW (general and top view).

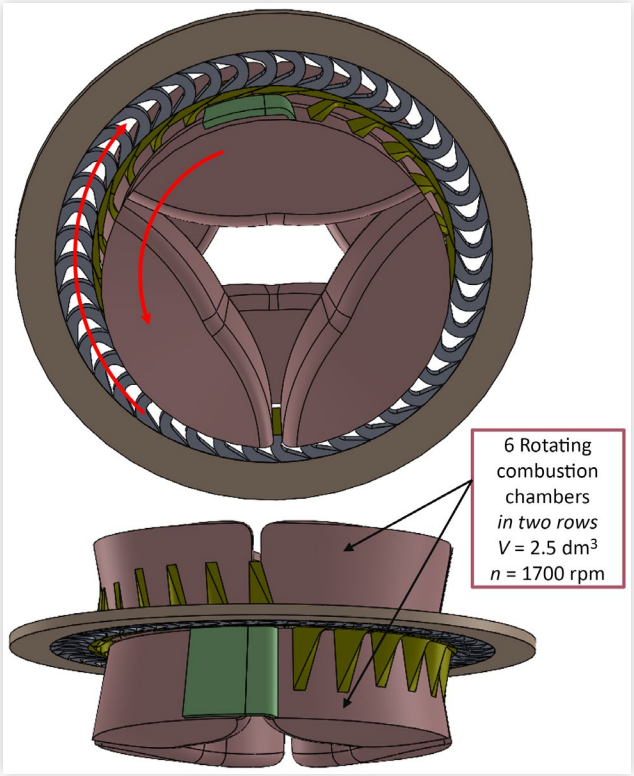

Moreover, a turbocharger was implemented, which uses the rest of the kinetic energy of gas behind the main gas turbine. Generation of power via turbine allowed simple and light construction.

Effective timing of the engine was ensured by the application of rotating combustion chambers (driven separately by an electric motor) and stationary inlet and outlet nozzles (see Figure 1). Such an arrangement brings several advantages:

- Only two sets of high-pressure (diesel) injection systems can be used,
- de Laval nozzles are stationary, so they are not loaded by centrifugal force. Only heat and gas pressure affect them, thus they can be made of ceramic materials,
- An effective ceramic sealing system can be applied to the rotating combustion chambers.

The rotation of the chambers enables the application of effective ceramic sealing. The segment sealing elements, working with counter-surface, can work via self-alignment, because of centrifugal forces acting on it. A quite low rotational speed of chambers (1379 rpm) ensures low loading of single-segment elements (4 N), resulting in low friction between the moving and stationary surfaces. The proposed system of seals ensures full chamber tightness, regardless of thermal conditions and related deformations because seals

FIGURE 3 Humphrey vs. Bryton–Joule cycle in *p*–*v* diagram.

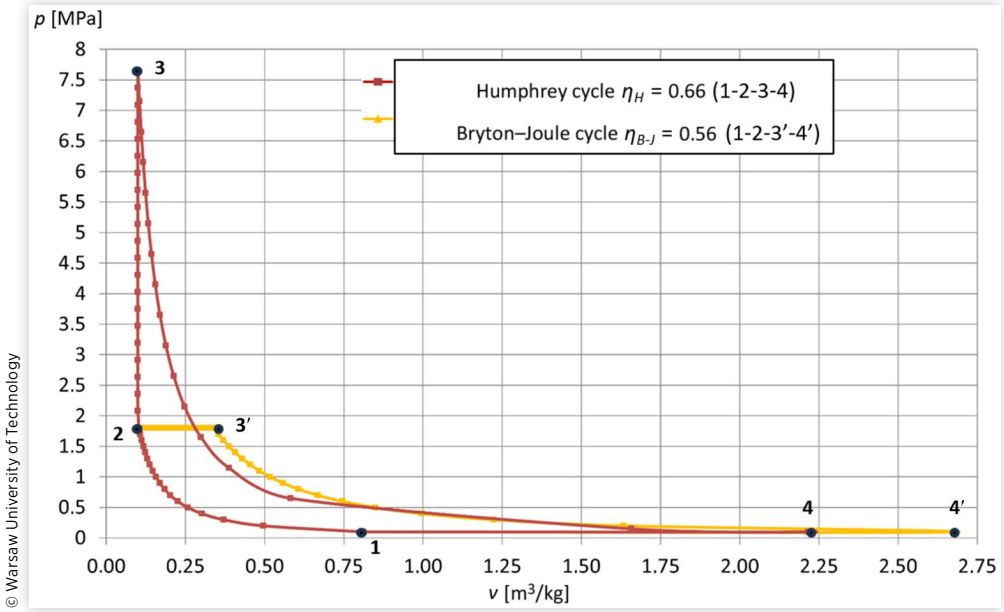

adapt to the size of the changing gap that occurs between chambers and counter-surface [9].

The effective expansion of gas was realized using four different de Laval nozzles. Due to the different operating pressures in the nozzles, they have different ratios of minimal to maximal cross-sectional area. Moreover, because of the different gas velocities in each de Laval nozzle, they are directed under different angles according to the turbine. The nozzles in conjunction with the radial turbine enabled smooth gas flow with low internal friction.

The hybrid concept of turboshaft engine as shown in [10] gives promising results of effective efficiency. Evaluated by CFD simulation, efficiency can differ from 0.33 to 0.37, depending on the generated power (463–1780 kW). The concept was built to face the performance of classical turboshaft engines existing on the market [11]. For example, the turboshaft engine AGT-1500, 1120 kW [1] (used in M1A2 Abrams tank), has an efficiency equal to 0.28. It can be noticed that the advantage of the calculated efficiency of the hybrid concept of turboshaft engine relative to the gas turbine working according to the Bryton–Joule cycle (AGT-1500, 1120 kW) is about 20%. Almost the same advantage was obtained by comparison of both ideal thermodynamic cycles.

A hybrid concept of turboshaft engines fits into the recently broadly investigated area of PGE (pressure-gained combustion) [12, 13, 14, 15, 16, 17, 18]. A lot of publications and efforts have been focused on the development of the radial wave engine (RWE), so it's worth noting some benefits of the proposed engine concept relative to RWE. The hybrid engine has a significantly smaller number of combustion chambers but with a larger volume. As a result, the filling process with fresh air lasts longer. The combustion chambers do not require perfect timing for closing and opening in the schedule of the engine cycle. Generally, the Humphrey cycle is easier to realize and it can be successfully done in a wider range of rotational speeds. The reason for this is the abandonment of additional compression using the phenomenon of a compression wave, which has a small effect. Next, the bigger size of combustion chambers allows for the implementation more robust sealing system, which is a critical point in the success of the entire engine concept. Moreover, the chambers need to be sealed on one side only, since inlet and outlet gases are flowing via the upper cylindrical surface. Finally, more efficient cooling of the combustion chamber can be applied compared to RWE.

The hybrid engine concept has the potential for practical implementation since it has a new idea of a sealing system. The ABB company [14] and California State Polytechnic University [16] failed. The common issue of the two failed attempts was not the resolved problem with the sealing of combustion chambers. Due to a lack of protection of the sealing idea applied in a hybrid engine concept, it is not shown in this article.

The article presents a variant of the hybrid concept of a turboshaft engine with partial turbine load. It is enhanced by a steam cycle with additional power generated by a steam turbine. The secondary steam cycle working according to Clausius–Rankine was supplied using waste heat recovery from cooling and the exhaust gas. The application of an additional steam cycle can improve significantly the effective efficiency of the engine.

Implementation of steam cycle installation (steam turbine, condenser, evaporator, water pump) will increase engine complexity and will decrease the power-to-mass ratio. Because of additional weight, it could have potential applications only for stationary use or heavy military boats or vehicles.

The following section presents a diagrammatic description of a complete engine with a combined cycle. The subsequent section presents CFD results of the hybrid concept of

turboshaft engines with the most important parameters. The fourth section contains detailed calculations of steam parameters in different cycle stages, which were based on CFD results. In the fourth section effective efficiency and specific fuel consumption of the engine are calculated. Finally, the conclusions are discussed.

2. Diagram of Combined Cycle Hybrid Concept of Turboshaft Engine

The proposed engine works according to two different thermodynamic cycles. The first one is the gas Humphrey cycle realized by a hybrid engine (left-hand side of Figure 4). The second one is the steam Clausius–Rankine cycle (right-hand side of Figure 2), which is realized by water pump, heat exchanger assembly, and steam turbine.

The gas patch starts at point 1 with atmospheric parameters. Then the gas is compressed in two compressor stages to the final value of 2.0 MPa (points 1–2 and 3–4) and cooled in an intercooler (points 2–3). Next isochoric combustion is realized (points 4–5). The energy of the high-pressure gas is transformed into mechanical energy in the turbine (points 5–6). The gas between points 6 and 7 gives back the rest of the kinetic energy in the turbocharger. Finally, heat recovery from the exhaust gas is used for steam production (points 7–8). The flow of the gas between points 4 and 6 was analyzed by CFD simulation, and the results are presented in the next section.

The steam patch starts at point 1′ where water is in a saturation state. Between points 1′ and 2′ the pressure of water is increased to 1 MPa in the pump. Next, water is heated up, evaporated, and overheated (points 2′–3′). Some portion of the heat is taken from the cooling of combustion chambers and nozzles. Most of the heat for the production of steam comes from the exhaust gas. The steam is expanded in the turbine between points 3′ and 4′. The steam changes the phase from steam to water in the condenser (points 4′–1′). The parameters of steam could be calculated based on CFD results. Detailed values are shown in the fourth section.

3. CFD Results of Hybrid Concept of Turboshaft Engine

The 3D numerical analysis contained a simulation of filling, direct injection of fuel, isochoric combustion, expansion, and mechanical power generation in the turbine. A transient set of Navier–Stokes equations, together with a compressible, semi-ideal energy equation, species transport, and reaction of combustion were resolved. The parameters of fuel injection

FIGURE 4 Diagram of the hybrid concept of turboshaft engine enhanced by steam cycle.

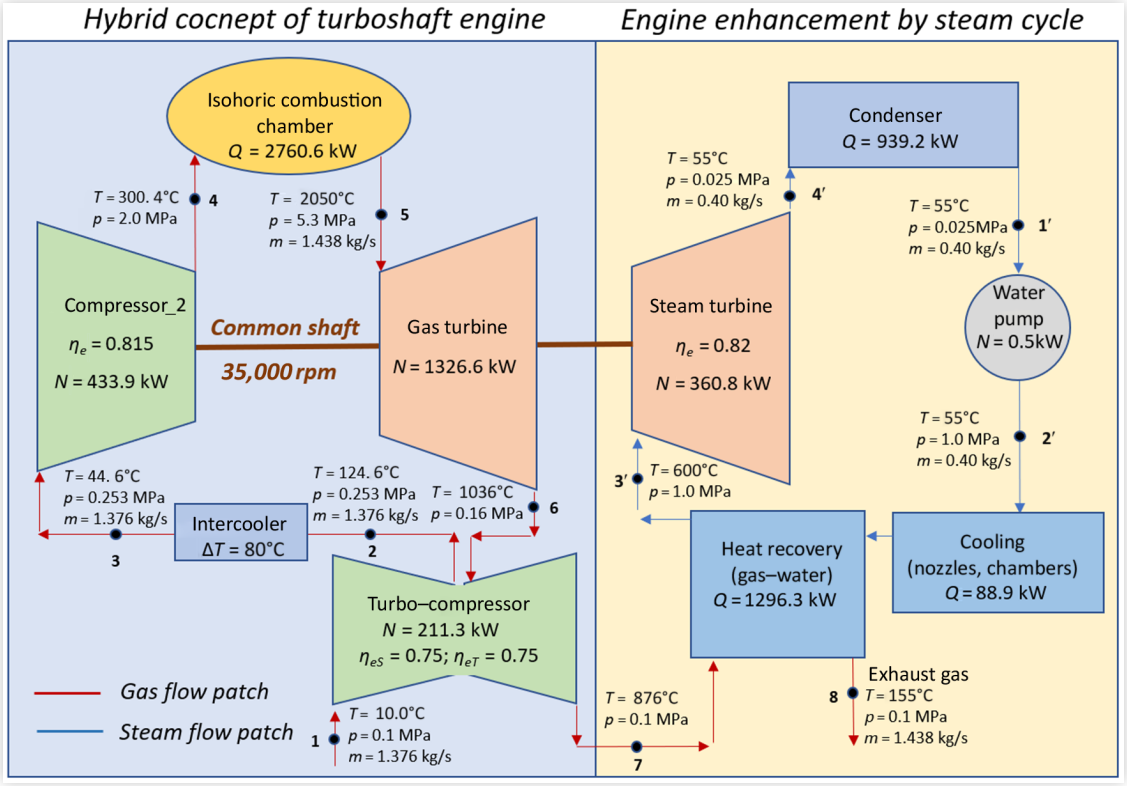

TABLE 1 Parameters of fuel injection used in the simulation.

Parameter	Value
Fuel	$C_{10}H_{22}$
Number of injectors	2
Type of injector	Cone 20°
Diameter of droplets	0.00016 m
Temperature of fuel injection	350 K
Velocity of fuel injection	330 m/s
Injection time	0.002 s
Interaction of droplets with gas phase	Dynamic drag, stochastic collisions, coalescence, breakup KHRT model
Combustion model	Eddy dissipation

are shown in Table 1. The thermal properties of gas species (specific heat, thermal conductivity, viscosity) were temperature-dependent. The commercial ANSYS Fluent software was employed for the analysis. The detailed numerical approach is given in [8, 9]. A simulation of the engine work was performed using a mesh consisting of 498,000 hexahedral elements (Figure 5). Due to the symmetry of the computational domain, a halved section of the model was simulated to reduce the computational load. The first element in the vicinity of the walls had a size of 0.25 mm. The mesh was created to assure y plus in the range of 30–300 value for most of the region. An enhanced wall treatment option was chosen to ensure the proper resolution of parameters in the boundary layer.

FIGURE 5 Simulation model of the hybrid concept of turboshaft engine (general and top view).

The left picture of Figure 6 presents the Mach number distribution. The highest value of 2.8 was reached at the end of the high-pressure nozzle. The right picture of Figure 6 presents pressure distribution in the vicinity of the blades. Integration of its values allowed the calculation of torque that is presented later, in Figure 10.

Figure 7 presents the results of oxygen content, and Figure 8 presents the temperature distribution for one cycle of the engine. The contents of chamber 1 are undergoing combustion while chamber 2 is being filled and chamber 3 is expelling its exhaust contents.

The gas pressure in the combustion chamber during filling has changed from 1.5 to 2.0 MPa. After combustion, the pressure increased to 5.3 MPa. Next, during expansion, the pressure decreased again to 1.5 MPa, where the next engine cycle started. The pressure change in three chambers and four nozzles is presented in Figure 9.

The torque generated in the turbine has changed from a minimum value of 130 Nm to a maximum value of 250 Nm (Figure 10). The values concerned the symmetrical half of the engine. The average torque for the entire model reached 381 Nm. The overall mass-averaged kinetic energy of the gas behind the main turbine has changed from 40 to 180 kW (Figure 11). The average value for the entire model reached 212.2 kW. It was used for supplying the turbocharger.

The chambers and nozzles were cooled to maintain the temperature on its inner surface equal to 1300°C [19]. It fulfilled the temperature requirements for ceramic coating materials. The average heat flux from the cooling of chambers reached 15.8 kW. The average heat flux from cooling nozzles was equal to 73.1 kW (Figure 12). The redundant heat supplied the steam cycle.

The average temperature of exhaust gas behind the turbocompressor was 876°C (Figure 13). Assuming its cooling by 721°C, it gave 1295.1 kW of heat power, which was used for steam generation.

4. Calculation of Steam Cycle Parameters

Details of the additional steam cycle (Clausius–Rankine cycle [20]) are presented in Figure 14. Complete evaporation of water was realized at 178°C, whereas condensation was at 55°C. The highest steam temperature was equal to 600°C.

The heat recovered from the exhaust was equal to 1295.1 kW. It was used for heating water, evaporation, and steam overheating as presented in Table 2. This constituted 46.95% of total combustion heat.

The mass flux of steam was equal to 0.375 kg/s. It was calculated based on Equation 1.

$$\dot{m}_p = \frac{Q_{rec}}{\Delta T_{\text{II–III}} C_p + i_{evap} + \left(i_{\text{V}} - i_{\text{IV}}\right)} \qquad \text{Eq. (1)}$$

FIGURE 6 Mach number distribution (left), static pressure distribution (right).

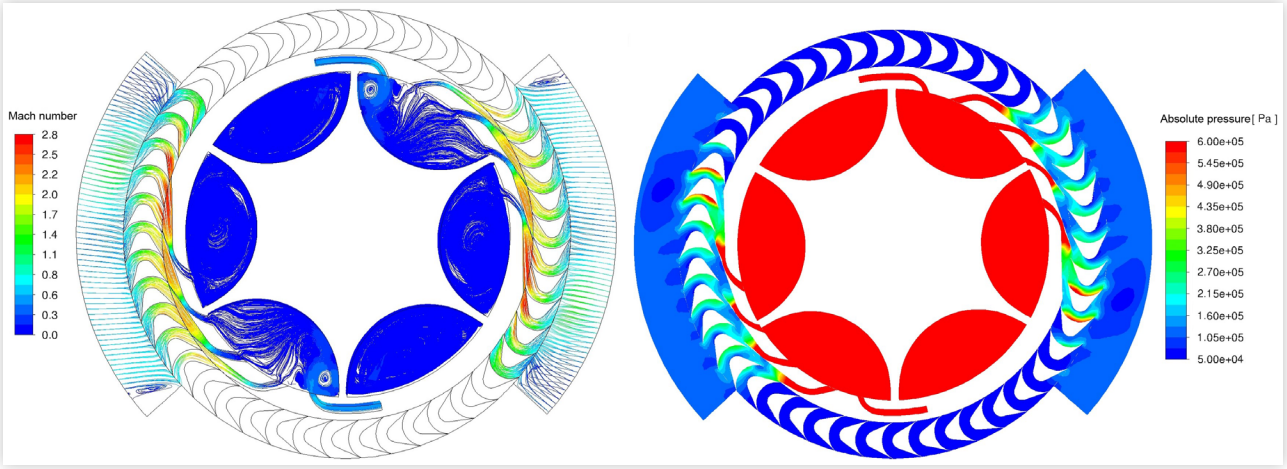

FIGURE 7 Change in oxygen content of the gas for 60 degrees of rotation of chambers (1 engine cycle).

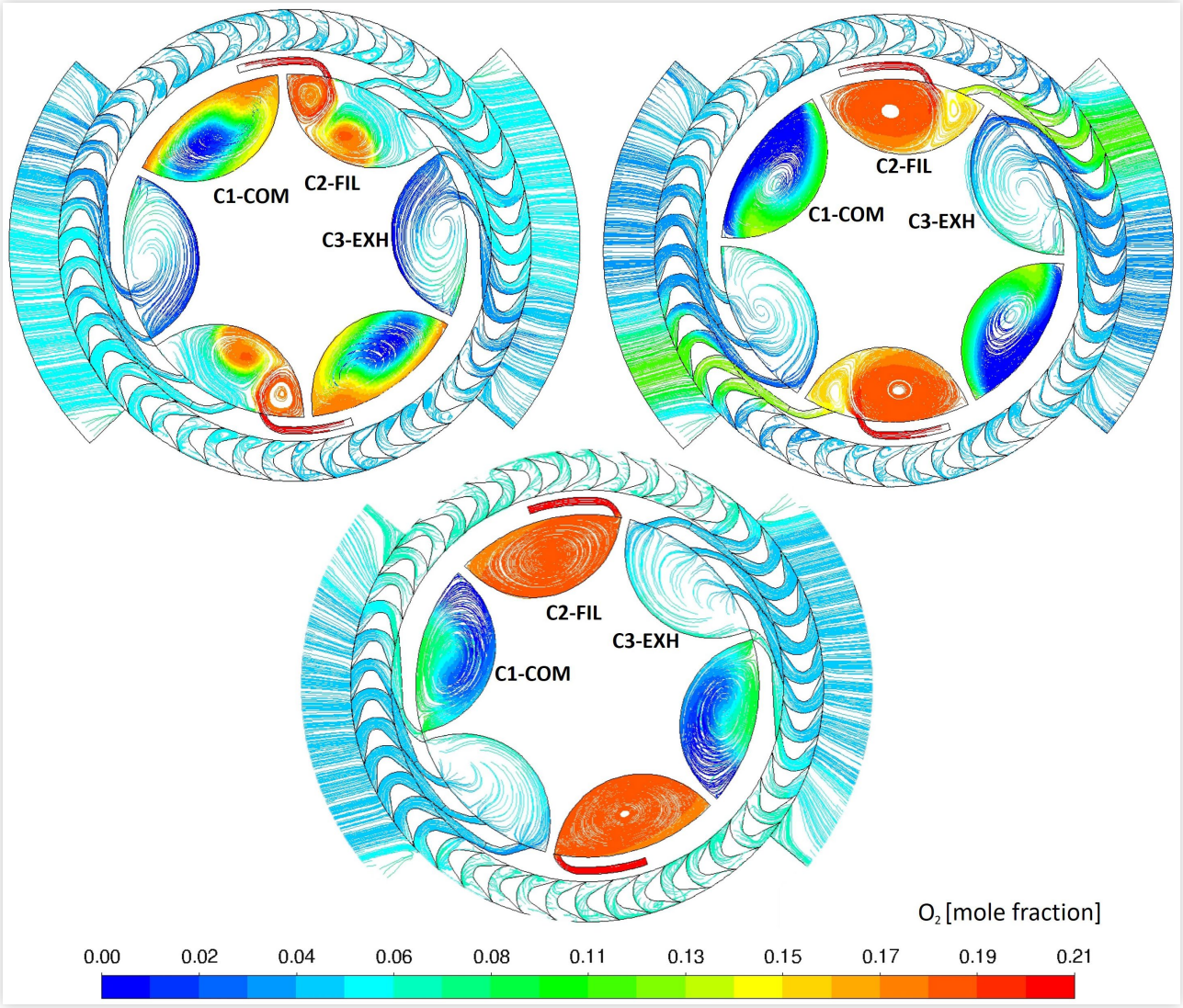

FIGURE 8 Change in temperature of the gas for 60 degrees of rotation of chambers (one engine cycle).

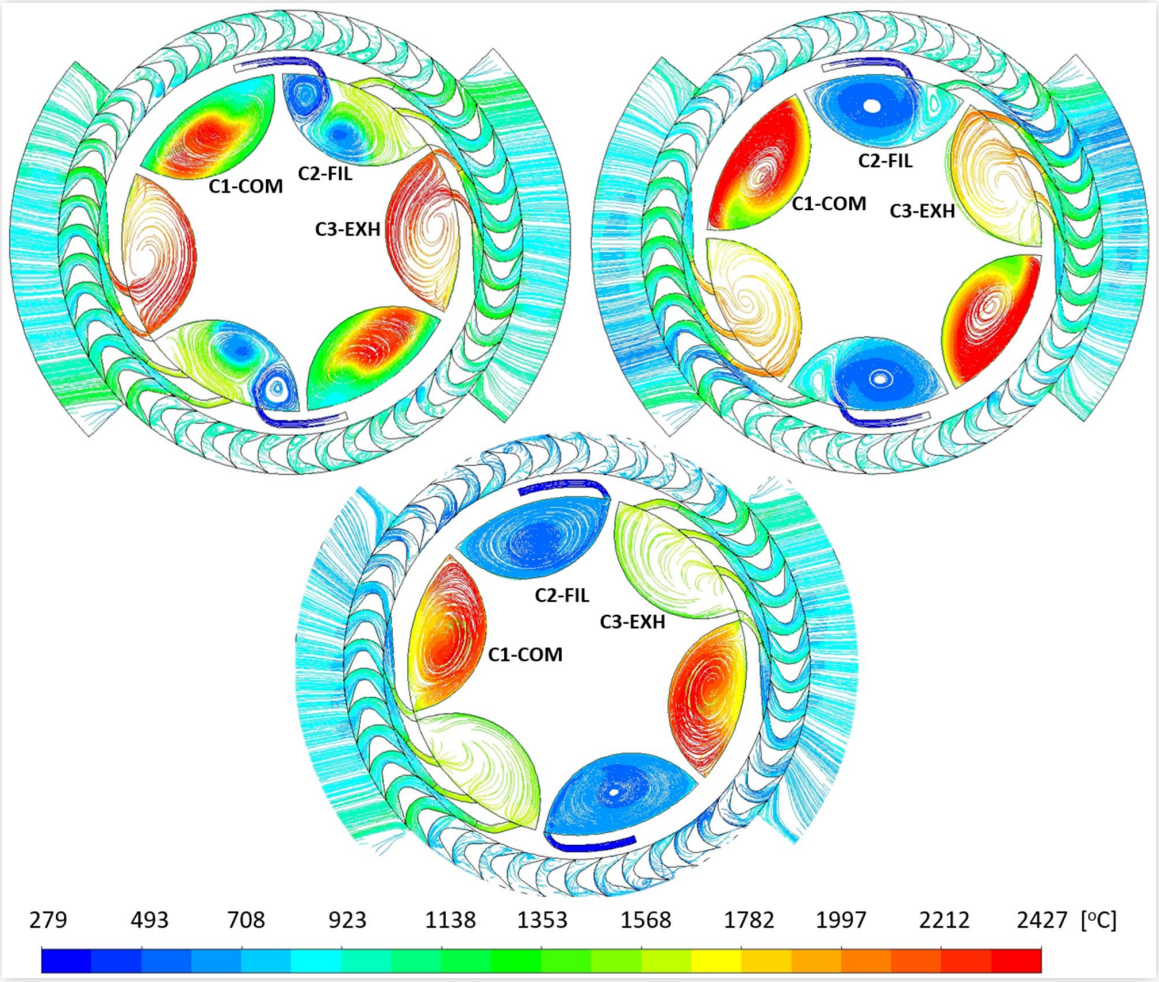

FIGURE 9 Pressure change of the gas in chambers and nozzles for two engine cycles.

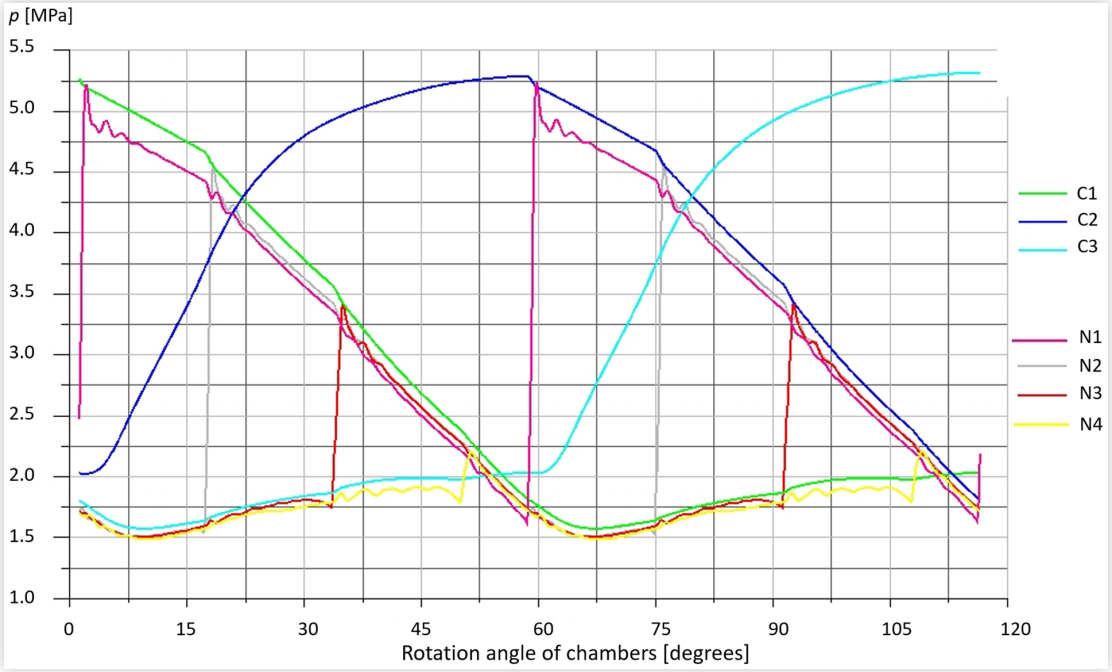

FIGURE 10 Torque generated in turbine for two engine cycles.

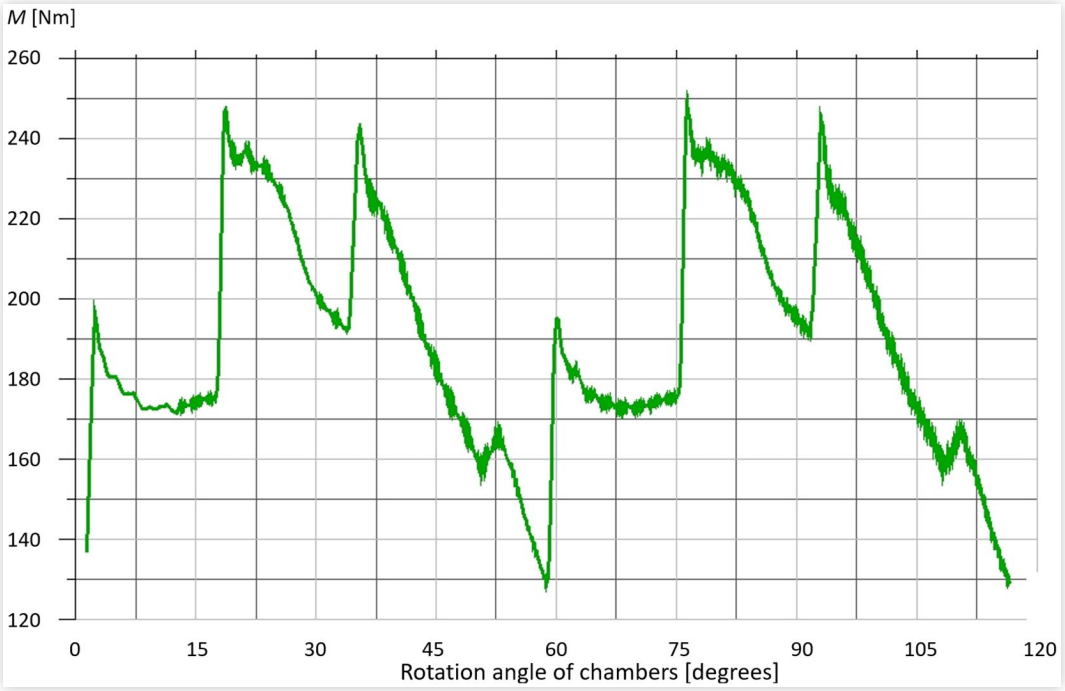

FIGURE 11 Kinetic energy of the gas behind the turbine for two engine cycles.

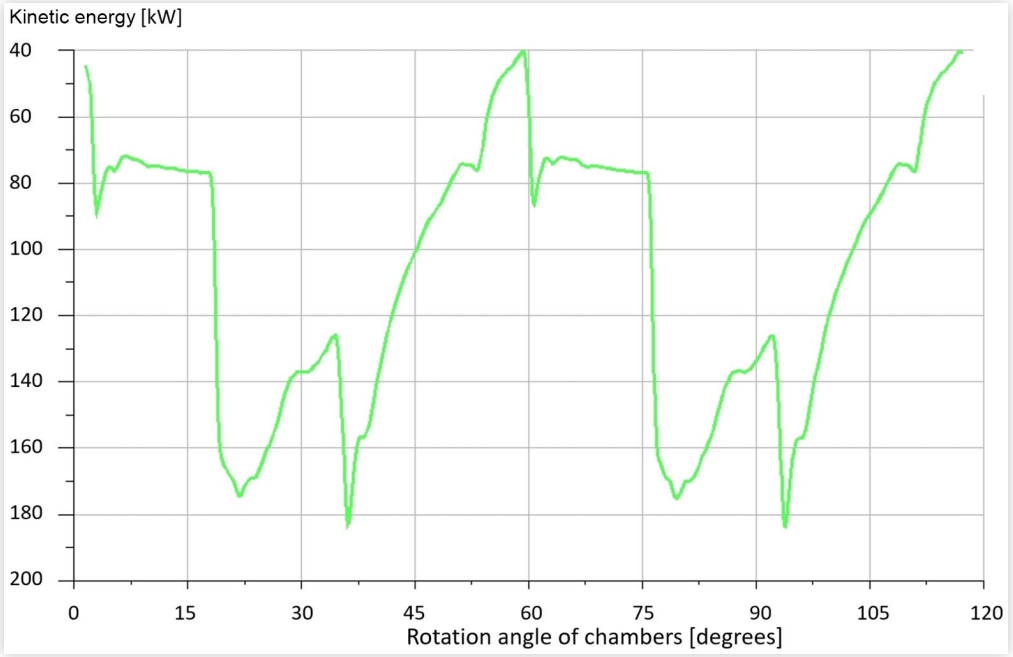

FIGURE 12 Heat of cooling for chambers and nozzles for two engine cycles.

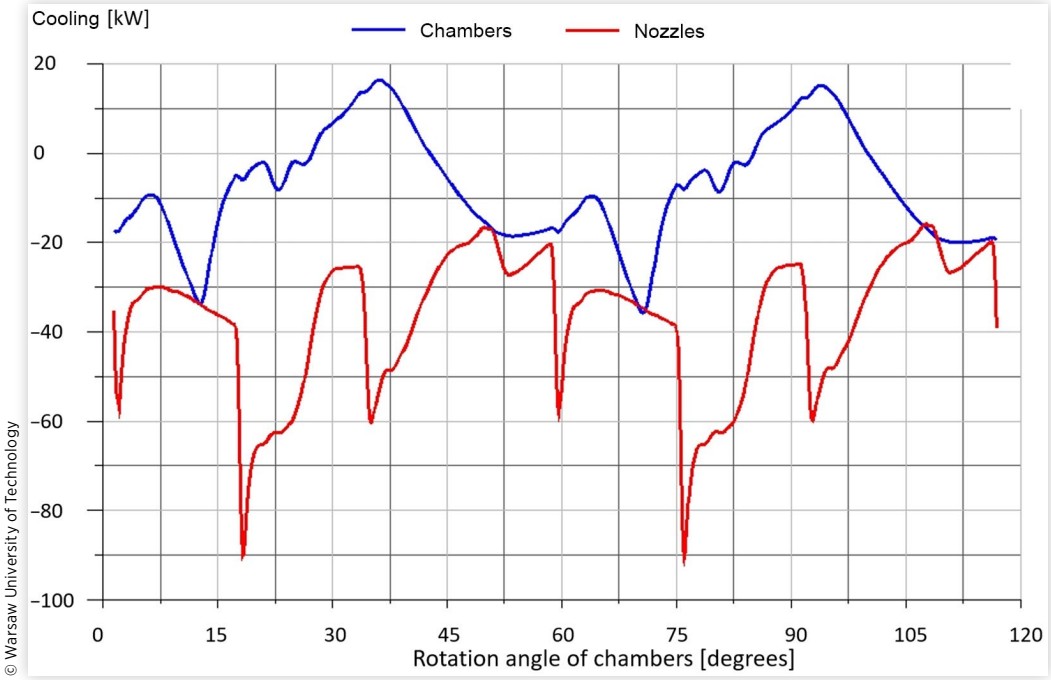

FIGURE 13 Temperature change of exhaust gas for two engine cycles.

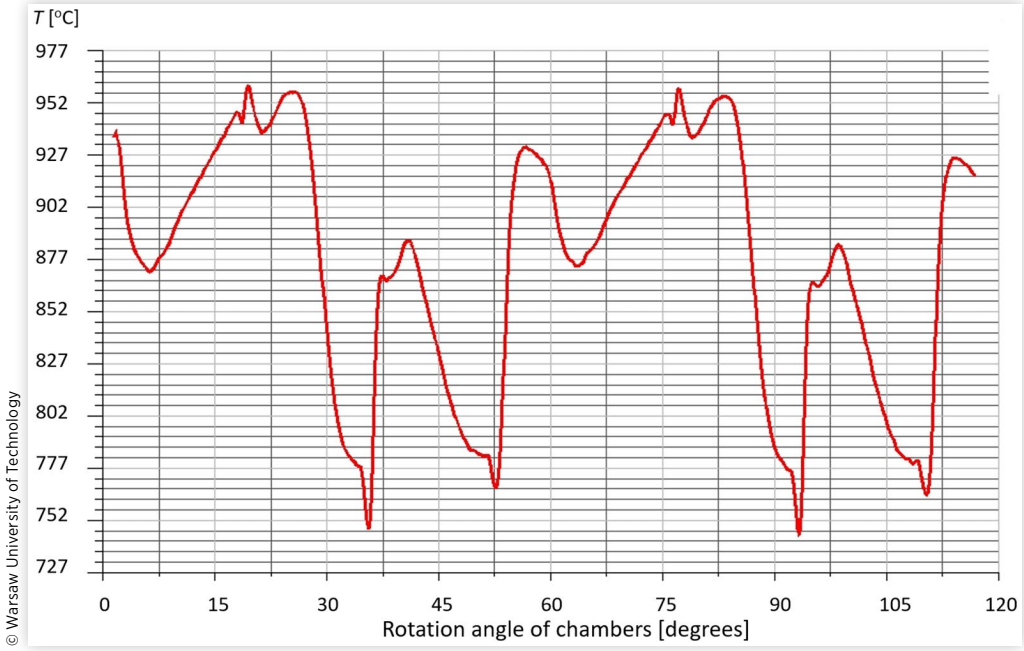

FIGURE 14 Steam cycle incorporated in the engine concept.

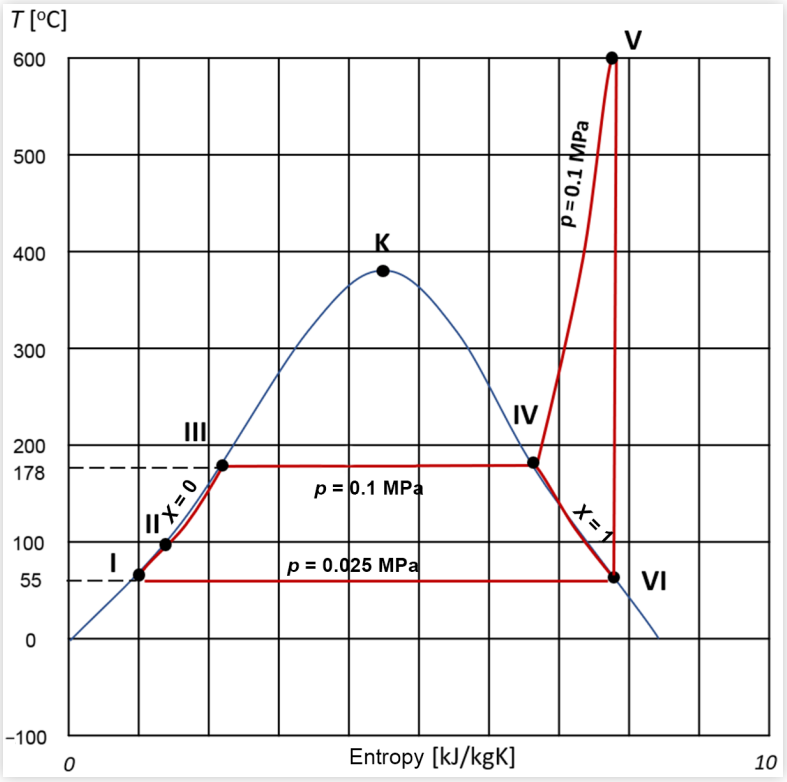

where $\dot{m}_p$ [kg/s] is steam mass flux, Q_{rec} [W] is heat recovery from cooling and exhaust gas, $\Delta T_{\text{II-III}}$ [°C] is change of water temperature during heating up, C_p [kJ/kg K] is water heat capacity, i_{evap} [kJ/kg] is enthalpy of evaporation (i_{evap} = 2013 kJ/kg), i_{IV} [J/kg] is enthalpy of saturated steam at point IV (i_{IV} = 2776 kJ/kg), i_{V} [kJ/kg] is enthalpy of overheated steam at point V (i_{V} = 3700 kJ/kg).

TABLE 2 Required heat for the steam cycle at different stages.

Operating points	Required energy [kW]	Share of recovered heat [%]
POINTS I–II water compression, Δp = 0.975 MPa	0.5	0
POINTS II–III water heating up, ΔT = 123°C	193.73	14.96
POINTS III–IV water evaporation, T = 178°C	754.9	58.29
POINTS IV–V steam overheating, ΔT = 422°C	346.5	26.75
POINTS V–VI steam expansion, Δp = 0.975 Pa	−412.6	−31.86
POINTS VI–I water condensation, T = 55°C, p = 0.025 MPa	−882.46	−68.14

5. Efficiency of Hybrid Concept of Turboshaft Engine Enhanced by Steam Cycle

The effective power generated by the gas turbine was equal to 1326.7 kW. It was determined from Equation 2.

$$N_{eGT} = \frac{M_{avg} \cdot n}{9549} \eta_{mTG} \qquad \text{Eq. (2)}$$

where N_{eGT} [kW] is effective power of gas turbine, M_{avg} [Nm] is averaged moment, n [rpm] is rotational velocity, 9549 = 60*1000/(2*π) is dimensionless unit converter, η_{mGT} is mechanical efficiency of the gas turbine (η_{mGT} = 0.95).

The effective power generated by the steam turbine was equal to 360.8 kW. It was calculated from Equation 3.

$$N_{eST} = \dot{m}_p \left(i_{\text{V}} - i_{\text{VI}}\right) \eta_{eST} \qquad \text{Eq. (3)}$$

where N_{eST} [kW] is effective power of steam turbine, i_{VI} [kJ/kg] is enthalpy of overheated steam at points VI (i_{VI} = 2600 kJ/kg), η_{eST} is efficiency of the steam turbine (η_{eST} = 0.82).

Using Equation 4 the effective power of engine reached 1253.5 kW

$$N_e = N_{eST} + N_{eGT} - N_{eMC} \quad \text{Eq. (4)}$$

where N_e [kW] is effective power of engine, N_{eMC} [kW] is mechanical power consumed by mechanical compressor.

The effective efficiency of engine reached 0.454. It was calculated from Equation 5.

$$\eta_E = \frac{N_e}{E_{chem}} \quad \text{Eq. (5)}$$

where η_E[-] is effective efficiency of engine, E_{chem} [kW] is power of chemical energy of fuel.

The final calculated parameter was specific fuel consumption. Based on Equation 6 it amounted to 179.2 g/kWh

$$g = \frac{m_{C_{10}H_{22}} \cdot 1000 \cdot 3600}{t_{cycle} \cdot N_e} \quad \text{Eq. (6)}$$

where g [g/kWh] is specific fuel consumption, $m_{10}H_{22}$ [kg] is mass of injected fuel, t_{cycle} [s] is time of single cycle of engine.

A summary of the calculated parameters of the presented engine concept is presented in Table 3.

TABLE 3 Characteristic parameters of the presented engine concept.

Parameter description	Value
The chemical energy of fuel	E_{chem} = 0.00024 kg·244, 240 kJ/kg/0.00769 s = 2760.6 kW
Effective kinetic energy demand for turbocharger (η_{eS} = 0.75; η_{eT} = 0.75) [21] p_2/p_1 = 2.53	N_{eTC} = 212.2 kW
Effective demand for power in mechanical compressor (η_{eS} = 0.815) [22] p_2/p_1 = 7.91	N_{eMC} = 433.9 kW
Effective power generated by gas turbine η_{mGT} = 0.95	N_{eTG} = [(381 Nm·35000 rpm)/9549]·0.95 = 1326.7 kW
Effective power generated by steam turbine η_{eST} = 0.82 [23]	N_{eTP} = 412.6·0.82 = 338.3 kW
Effective power generated by engine	N_e = 1326.7 + 338.3 – 433.9 = 1231.3 kW
The effective efficiency of the engine concept	η_E = 1231.3/2760.6 = **0.446**
Specific fuel consumption	g = 2·0.00024·1000·3600/(0.00769·1231.3) = 182.4 g/kWh

6. Conclusions

The article presents a merged analytical–numerical CFD analysis of the hybrid concept of turboshaft engine enhanced by steam cycle using waste heat recovery. The engine concept reached a very promising 0.446 of effective efficiency and 182.4 g/kWh of specific fuel consumption.

It exceeds the parameters of turboshaft engines and piston engines existing on the market for similar power. For example, the turboshaft engine AGT-1500 [1] (used in M1A2 Abrams tank), 1120 kW has η_e = 0.28 and g = 305.9 g/kWh. The piston engine MTU 883 Ka-501 (used in Leopard 2 tank), 1200 kW has η_e = 0.397 and g = 215.0 g/kWh [24].

However, the parameters obtained from the merged numerical and analytical calculation should be treated with some caution. Because of inherent simplifications of analytical and simulation calculation margin error is possible. Nevertheless, the achievement proposed a unique engine concept with very good operating parameters both in the gas cycle version of the engine and in the combined cycle version of the engine. The next step should be to experimentally check the tightness of the combustion chambers using a system of self-adjusting ceramic seals.

Implementation of the installation of the steam cycle (steam turbine, condenser, evaporator, water pump, and mass of water) will increase engine complexity and will decrease the power-to-mass ratio coefficient. Nevertheless, it is believed that it can be still successfully applied to vehicles because of the light and simple construction of the primary gas engine. Even though the presented engine concept could have the same power-to-mass ratio coefficient as the piston engine, it would still have an advantage because of the application of the turbine, which guarantees better dynamics of the vehicle. This is very important in the case of tanks on the battlefield.

It is worth underlining that the centrifugal compressor, gas turbine, and steam turbine can work on the common shaft, which simplifies the construction. Its rotational velocity can be in the range of 35,000 rpm.

The very low temperature of exhaust gas at 155°C is beneficial, especially for military applications because this would render the vehicle difficult to recognize by infrared radars.

Contact Information

Piotr Tarnawski, corresponding author
piotr.tarnawski@pw.edu.pl

References

1. Mazuro, P. and Chmielewski, C., "Military Vehicle Options Arise from the Barrel Type Piston Engine," *Journal of Power Technologies* 101, no. 1 (2021): 22-23.
2. Walentynowicz, J., "Propulsion Motors for Combat Vehicles," *Journal of KONES WAT Powertrain and Transport* 13, no. 4 (2006): 129-140.

3. Tarnawski, P., "Analytical Performance Evaluation of Humphrey Cycle for Turbine Engine Application," *Machine Dynamics Research* 41, no. 3 (2017): 27-37.
4. Tarnawski, P. and Ostapski, W., "Pulse Powered Turbine Engine Concept – Numerical Analysis of Influence of Different Valve Timing Concepts on Thermodynamic Performance," *Bulletin of the Polish Academy of Sciences* 66, no. 3 (2018): 373-382, doi:https://doi.org/10.24425/123444.
5. Tarnawski, P., "Pulse Powered Turbine Engine Concept," Doctoral dissertation, Warsaw University of Technology, Warsaw, 2018.
6. Tarnawski, P. and Ostapski, W., "Pulse Powered Turbine Engine Concept Implementing Rotating Valve Timing System: Numerical CFD Analysis," *Journal of Aerospace Engineering* 32, no. 3 (2018): 04019017.
7. Tarnawski, P. and Ostapski, W., "Turbine Engine Concept Realizing Humphrey Cycle," in Mazurkow A. (ed.), *Materials, Technologies, Constructions – Constructions and Design*, Vol. 4 (Rzeszow, Poland: Rzeszow University of Technology, 2019), 23-43.
8. Tarnawski, P. and Ostapski, W., "A Concept of a Pulse-Powered Turbine Engine with Application of Self-Acting Displacement Valves—3D Numerical Analysis," *SAE Int. J. Engines* 14, no. 3 (2021): 419-437, doi:https://doi.org/10.4271/03-14-03-0025.
9. Tarnawski, P. and Ostapski, W., "Rotating Combustion Chambers as a Key Feature of Effective Timing of Turbine Engine Working According to Humphrey Cycle – CFD Analysis," *Bulletin of the Polish Academy of Sciences* 70, no. 5 (2022): e143100, doi:https://doi.org/10.24425/bpasts.2022.143100.
10. Tarnawski, P., "The Hybrid Concept of Turboshaft Engine Working According to Humphrey Cycle Dedicated to Variety Power Demand – CFD Analysis," *Combustion Engines* 193, no. 2 (2023): 129-136, doi:https://doi.org/10.19206/CE-162763.
11. Litalien, C., "Pratt and Whitney Canada Turboshaft Engines Product and Technology Evolution," in *European Rotorcraft Forum 33*, Kazan, Russia, 2007.
12. Brophy, C. and Roy, G., "Benefits and Challenges of Pressure-Gain Combustion Systems for Gas Turbines," *Mechanical Engineering* 131, no. 3 (2009): 54-55, doi:https://doi.org/10.1115/1.2009-MAR-8.
13. Kurec, K., Piechna, J., and Gumowski, K., "Investigations on Unsteady Flow within a Stationary Passage of a Pressure Wave Exchanger by Means of PIV Measurements and CFD Calculations," *Applied Thermal Engineering* 112, no. 5 (2017): 610-620, doi:https://doi.org/10.1016/j.applthermaleng.2016.10.142.
14. Akbari, P. and Nalim, M.R., "Review of Recent Developments in Wave Rotor Combustion Technology," *Journal of Propulsion and Power* 25, no. 4 (2009): 833-844, doi:https://doi.org/10.2514/1.34081.
15. Walraven, F., "Operational Behavior of a Pressure Wave Machine with Constant Volume Combustion," ABB Technical Report CHCRC 94-10, 1994, Tatarstan, Russia, September 11–13, 2007.
16. Akbari, P., Tait, C., and Brady, G., "Enhancement of the Radial Wave Engine," in *AIAA Propulsion and Energy 2019 Forum*, Cincinnati, August 2019.
17. Piechna, J., "A Review of Shock Wave Compression Rotary Engine Projects, Investigations and Prospects," *Energies* 15, no. 24 (2022): 9353, doi:https://doi.org/10.3390/en15249353.
18. Batista, A., Ross, M.C., Lietz, C., and Hargus, W.A. Jr., "Descending Modal Transition Dynamics in a Large Eddy Simulation of a Rotating Detonation Rocket Engine," *Energies* 14 (2021): 3387, doi:https://doi.org/10.3390/en14123387.
19. Derlukiewicz, D., "Method of Modeling of Thermo-Elastic Phenomena in Layered Ceramic Coatings," Doctoral dissertation, Wroclaw University of Technology, Wroclaw, 2006.
20. Dowkontt, J., "Theory of Thermal Engines," Communications publisher (pol. Wydawnictwo Kmunikacji i Łączności), 1973.
21. Turbo Tech 103 Expert, "Compressor Mapping," accessed December 10, 2020, www.garrettmotion.com/wpcontent/uploads/2019/10/GAM_Turbo Tech-103_Expert-1.pdf.
22. Rodgers, C., "The Efficiencies of Single-Stage Centrifugal Compressors for Aircraft Applications," The American Society of Mechanical Engineers, New York, 1991, accessed July 11, 2017, https://proceedings.asmedigitalcollection.asme.org.
23. Kryłoiwcz, W. and Kabałyk, K., "Low-Power Steam Turbines for Distributed Energy – State of the Art, Domestic Experience and Implementation Capabilities," INSTAL 4/2020, 2020, 12-16, https://doi.org/10.36119/15.2020.4.2
24. Land Defense, "MTU Partner for Unrivaled Solutions," MTU-Defense-brochure.pdf, 2016, https://svf-international.com/mexico/wp-content/uploads/sites/5/2016/05/MTU-Defense-brochure.pdf.